DESIGN AND MANUFACTURING OF TORSIONAL FLEXIBLE BLADE MODELS

F. Dupriez, P. Geoffroy, B. Paluch
Institut de Mécanique des Fluides de Lille
IMFL - ONERA
5, Boulevard Paul Painlevé - 59000 Lille
France

Abstract

This paper concerns manufacturing and design of instrumented blade models with specified torsional flexibility and straight removable tip, which will be tested in ONERA Chalais wind-tunnel. The purposes are to take into account the torsional deformation of the blades in order to increase helicopter's rotor performance, and to improve and fit the calculation codes relative to aeroelastic deformations and aerodynamic loads during hover and forward flight. An iterative procedure is employed to determine the blade's internal distribution of composite material layers, and to obtain a value of tip end torsion angle close to +/- 3° during a rotation. Six material configurations are tested before a good agreement is found. To avoid strong couplings between modeshapes, this removable blade-tip joint is realized with two specific metallic inserts. The blades are instrumented with a particular strain gauges disposition, in order to measure their deflection during wind-tunnel tests.

Notation

$[A_{str}]$	Structural damping matrix
$[A_{aero}]$	Aerodynamic damping matrix
$[B]$	Generalized damping matrix
$\{F_{str}\}$	Structural loads vector
$\{F_{aero}\}$	Aerodynamic loads vector
$\{F(t)\}$	Generalized centrifugal loads vector
$[K]$	Stiffness matrix
$[K_{str}]$	Structural stiffness matrix
$[K_{aero}]$	Aerodynamic stiffness matrix
$[M]$	Generalized mass matrix
$\{Q(t,q,..)\}$	Generalized aerodynamic loads vector
$\{Y\}$	Displacement vector
$\{\dot{Y}\}$	Velocity vector
$\{\ddot{Y}\}$	Acceleration vector
$a_0,a_1,...$	Harmonic coefficients of torsional deflection
c	Blade chord (m)
C_z	Lift coefficient
M	Mach number
P	Rotor thrust (kW)
R	Rotor radius (m)
R_0	Blade root radius (m)
R_t	Blade-tip joint radius (m)
$s(t)$	Generalized coordinates of the blade
V	Forward flight speed (m/s)
$\overline{X}$	Rotor propulsive force coefficient
$\overline{Z}$	Rotor lift force coefficient
α_q	Rotorshaft tilt angle (deg)
$\beta(t)$	Rigid blade flapping angle
$\delta(t)$	Rigid blade lag motion
ϕ	Local incidence angle of the blade (deg)
Ω	Nominal rotational speed of the rotor (rad/s)
Ψ	Blade azimuth (deg)
θ_0	Collective pitch (deg)
μ	Advance ratio
σ	Solidity ratio

Introduction

In the framework of the ROSOH operation conducted jointly by AEROSPATIALE and ONERA, the IMFL is given the task of designing and manufacturing torsional flexible blade models with removable straight tips. These blades are actually tested on the three-bladed rotor facility of the Chalais-Meudon S2 wind-tunnel (Fig 1). The main goal of this operation is to take the torsion blade deformation into account in the design of helicopter rotors to increase their performances as it seems possible (Ref 1). An other point is to improve the methods used to calculate aeroelastic deformations, dynamic loads and stability in forward and hovering flight.
The main specification concerning the blades is to obtain a tip end torsion deformation angle of about +/- 3°, for the following flight conditions (s1) :

Ω=245 rd/s
$\overline{Z}$=13.3
$\overline{X}$=1.52
μ=.39
σ=0.137
V=82 m/s

The torsional eigenfrequency must be also near 3Ω (s2)

Description of the blade geometry

The main dimensions of the blades are :

R_0=0.177 m
R_t=0.677 m
R =0.857 m
c =0.123 m

with an OA209 aerodynamic profile.
The internal structure (Fig 2) of the composite blade is made up of :

- cross-ply composite material skins
- unidirectional R glass/epoxy rear and front spars
- low density foam filler
- aluminum tab attached to the rear spar, to adjust previously the imposed conditions mentionned above, during wind-tunnel tests.

The blade-tip joint is conceived to avoid coupling effects between modeshapes and to have nodal lines as pure as possible. The adjustment of the torsional eigenfrequencies, related to the tip end torsional deformation, is carried out by successive modifications of the composite material stacking sequences constituting the skin.

Vibration Analysis

In this section, the computational methods for the prediction of natural frequencies and mode shapes of the blades, at rest and in rotation, are presented. Further, numerical results obtained for various material skin configurations are reported and will be discussed with respect to the rotor design specifications.

Finite Element Discretization of the Blade at Rest

Owing to the slenderness (length/thickness) and chordwise (length/chord) ratios approximatively equal to 70 and 5 respectively, the free-vibration analyses of the blade model are carried out using a thick degenerate three-dimensional multilayer element implemented in the ONERA's linear finite element code ASTRONEF (Ref 2).

Finite Element Model

The composite thick shell element is quadrilateral, isoparametric, and has curved faces. This element formulation is derived from the twenty nodes isoparametric element formulation, and includes mean transverse shear. The specific hypotheses are a stress $\sigma_{zz} \tilde{=} 0$ and a linear variation of the displacements through the thickness. For more details about this formulation, see Refs 3, 4, 5, and 6. The element (Fig 3) has eight nodes, with five degrees of freedom per node: three displacement vector components $\{u,v,w\}$ and two rotations $\{\alpha,\beta\}$ of the unit vector $\vec{V_3}$ about the unit vectors $\vec{V_1}$ and $\vec{V_2}$. The method used to determine the blade model eigenfrequencies and eigenvectors is based on the classical subspace iteration algorithm, where the first p eigenmodes, associated to the first p eigenvalues, are calculated in a given frequential domain (Ref 7).

Finite Element Modelisation

The mesh considered for the eigenfrequency calculations has respectively nine and nineteen divisions in the chordwise and the spanwise directions. The blade root is divided in five sections to take into account the large evolution of thickness, chord and internal material distribution in this area. Let us note that the removable tip joint is modelised with three sections. As shown in Fig 4a, the final mesh leads to 555 nodes, 332 elements, and consequently 2,775 d.o.f. . The imposed boundary conditions correspond to a clamped blade root.

Determination of Dynamic Characteristics in Rotation

An aeroelastic code, developed by the ONERA Structures Department for stability problem investigations concerning helicopter rotors (Ref 8) and high speed propeller blades (Ref 9), is used to obtain the vibrational characteristics of the rotating blades. This program is based on the resolution of the following system of differential equations :

$$[M]\{\ddot{Y}\}+([A_{str}]+[A_{aero}])\{\dot{Y}\}+([K_{str}]+[K_{aero}])\{Y\}=\{F_{str}\}+\{F_{aero}\}$$

The blade, modelised as a beam, has an elastic axis assumed to be located on the first quarter of the chord. The aeroelastic behaviour of the rotor blades is described by using the complete blade natural vibration mode components at rest. A linear 2D aerodynamic model is implemented, and can be expressed as :

$$C_z = \frac{2\pi\phi}{\sqrt{1-M^2}}$$

Numerical Results and Discussion

According to the specified conditions (s1) (s2), the following six different stacking sequences of composite material associations are studied :

(a) four satin woven E glass/epoxy plies over the whole span
(b) four UD E glass/epoxy plies [+45°/-45°/+45°/-45°] over the whole span
(c) same material as in (b) with [+30°/-30°/+30°/-30°]
(d) same material as in (b) with [0°/90°/0°/90°]
(e) four UD E glass/epoxy plies along the main part of the blade, and four satin woven Glass/epoxy plies for the removable tip.
(f) three UD E glass/epoxy plies [0°/90°/0°] plus a satin woven E glass/epoxy for the main part, and four satin woven E glass/epoxy for the tip.

At rest, considering all the numerical results, we observe that the mode shapes are pure and uncoupled. Especially the torsional nodal line is located on the 30 % chord axis. This can be explained from the fact that the retained design solution for the removable blade tip joint is correctly adjusted. For example, the first torsional mode obtained with the case (f) is shown on Fig 4b.

In rotation, the numerical vibration analysis is carried out in vacuum, with a blade setting angle equal to zero.

Table 1 lists the numerical values of the reduced torsional frequency (ω/Ω) calculated for Ω and for the six material configurations.

	Reduced frequency
Case (a)	2,39
Case (b)	3,68
Case (c)	3,5
Case (d)	2,89
Case (e)	2,92
Case (f)	2,74

Table 1 : Numerical values of the reduced torsional frequency for the cases (a) to (f).

Figures 5 and 6 show the variations of the first five natural frequencies as functions of rotational speed, calculated for the cases (b) and (f) respectively. In a general manner, the second and third flapping frequencies as functions of the rotational speed increase whereas the torsion mode increases slightly.
The torsion frequency value found in case (a) is too weak compared to the imposed specifications, so this case is discarded. For the case (b) the third flapping mode crosses the torsion mode near Ω. A crossing also appears in the case (c). Furthermore, the solutions (b) and (c) are unacceptable in comparison with stability.
The reduced torsional frequency obtained with the case (e) is too close to 3Ω, consequently case (e) is not retained. Only cases (d) and (f) give preliminary acceptable solutions.

Calculation Method for Rotor Dynamic Response in Forward Flight

A specific aeroelastic calculation code called PAP, also developed at ONERA (Ref 10), is used to predict the dynamic response of helicopter rotor blades in forward flight. This program calculates the forced response and the dynamic hub loads. Its formulation is based on a modal approach coupled with a quasi-steady or a non linear unsteady aerodynamics. The resolution of the set of the following second-order differential equations with periodic coefficients:

$$[M]\{\ddot{q}(t)\}+[B]\{\dot{q}(t)\}+[K]\{q(t)\}=\{F(t)\}+\{Q(t,q,\dot{q},\ddot{q})\}$$

where the vector $\{q(t)\}$ is defined as :

$$<q(t)>=<\beta(t),\delta(t),s(t)>$$

gives the non linear response of the rotor blade motion. The flow field is assumed as two-dimensional for all local rotor blade sections. For the quasi-steady aerodynamic calculations, the section lift, drag, and pitching moment coefficients are raised from static airfoil data tables. The non linear unsteady aerodynamics adopted in PAP program is the semi-empirical dynamic stall model (Refs 11, 12). Induced velocity over the rotor disc is calculated by using the Meijer-Drees model. At least, step-by-step explicit integration scheme is employed to solve the set of differential equations mentioned above.

The blade structural and dynamic characteristics are supplied, including mass, stiffnesses and inertial properties distributions, and eigenfrequencies with their associated eigenmodes at rest. The two rigid blade modeshapes (flapping and lead-lag), and the three flexible modeshapes (first two flapping and first torsion eigenmodes) are introduced in the modelisation. In order to ensure the results convergence to the periodic solution, the analysis is carried out with 40 revolutions of the three bladed-rotor. Table 2 gives the numerical values of the rotor thrust, flight commands (shaft tilt angle and collective pitch), and harmonic coefficients of the tip end torsional deflection, obtained for the cases (d) and (f) with a quasi-steady aerodynamics.

	Case (d)	Case (f)
P	30	31,3
α_q	-18,6	-18,8
θ_o	20,9	21,2
a_o	-0,06	-0,28
a_1	1,92	2,27
a_2	1,1	1,6

Table 2 : Numerical values of the rotor thrust, flight commands and harmonic coefficients of the tip end torsional deflection, for the cases (d) and (f).

Fig 7 shows the evolution of the tip end torsional deflection as a function of the blade azimuth for one complete revolution, calculated for the retained case (f). We can see that for this case, the greatest amplitude of the first harmonic coefficient of the tip end torsional deformation is obtained. Note that the half peak-to-peak value of end tip torsional deformation is about of 3.3 degrees (Fig 7). This result can be partially explained by the fact that the value of natural blade torsion frequency for this case is the smallest one.
Figures 8, 9 and 10 exhibit lift coefficient, local incidence and pitching moment coefficient contours over the rotor disc, for the selected case. Note also that the negative lift coefficients appear near the tip on the advancing blade side, and are associated to the negative local incidences.

Blade Instrumentation

In order to establish an experimental data base for the comparison with the computed results, the blades are instrumented to measure the aeroelastic deformations in rotation during wind-tunnel tests. This instrumentation consists of strain gauge surveying bridges and 24 strain

gauges bridges (4 on tip and 20 on main part) distributed along the spanwise array between r/R=0.286 and r/R=0.977 as shown on Fig 11. These bridges measure the aeroelastic deformations during wind-tunnel tests, using Strain Pattern Analysis method (Ref 13). They are wired to have responses which are alternatively the sums or the differences of the flapping and torsion deformations. Moreover, in order to preserve the surface of the external blade skin and to dissociate the instrumentation phase from the other phases of manufacturing, the strain gauges are setted inside the skin before the curing of the entire model (Ref 14). The bridges responses are calibrated by measuring the output at four steady flexural and torsional moments. The corresponding bridge sensitivities are plotted on Fig 12, and have to be compared to the evolutions of flapping and torsional rigidities.

Concluding remarks

Actually the wind-tunnel tests are in progress, and the comparison between the experimental and the calculation results will be presented in a next paper.
However, vibration tests of the blades at rest show a very good agreement between the measured and computed values of the eigenfrequencies and modeshapes.
From a numerical point of view, the specified tip end torsional value is reached, and the first harmonic coefficient of the torsional deflection is in the required range of 2-3 degrees.
At least, the practical design difficulty was to minimize the influence of the blade-tip joint on the eigenmode couplings. This difficulty was get over by logging two compact and separated high strength steel inserts. This solution was successfully tested in fatigue.

References

1. Mantay W.R. , Yeager W.T. , "Aeroelastic considerations for torsionnaly soft rotors", AHS paper, February 1985

2. ASTRONEF, "Analyse des Structures à l'ONERA par Elements Finis", Set of finite element programs developed at the Structural Mechanics Department on UNIVAC 1110 computer

3. Simon L. ,"A set of finite elements developed for the dynamic computation of composite helicopter blade", Internal Conference on Composite Structures, Paisley (G.B.), 1981

4. Girard R. ,"Dynamical Vibrations of rotating laminated composite structure", La Recherche Aérospatiale, N° 1986-2, pp. 46-54

5. Geoffroy P. , "Numerical determination of the dynamic characteristics of a composite blade", La Recherche Aérospatiale, N° 1986-2, pp. 55-62

6. Dupriez F., Geoffroy P., Paluch B., "Design and manufacturing of composite materials blade models", 14th European Rotorcraft Forum, Milano (Italy), September 1988, paper N° 101, 21 pages

7. Osmont D., Simon L., "Un algorithme d'itération sur le sous-espace pour le calcul des modes propres de systèmes gyroscopiques", La recherche Aérospatiale, N° 1981-3, pp. 197-202

8. Costes J.J., Nicolas J., Petot D., " Etude de la stabilité d'une maquette de convertible", La Recherche Aérospatiale, N° 1982-6, pp. 413-440

9. Petot D., Besson J.M., "Comportement dynamique d'un prop-fan", Symposium on Aerodynamics and Acoustics of Propellers, AGARD/FDP , Toronto (Canada), October 1984

10. Peleau B., Petot D., "Aeroelastic prediction of rotor loads in forward flight", 13th European Rotorcraft Forum, Arles (France), September 1987, paper N° 6-4

11. Petot D., "Progress in the semi-empirical prediction of the aerodynamic forces due to large amplitude oscillations of an airfoil in attached or separate flow", 9th European Rotorcraft Forum, Stresa (Italy), September 1983

12. Tran C. T., Petot D., "Semi-empirical model for the dynamic stall of airfoils in view of the application to the calculation of responses of a helicopter blade in forward flight", 6th European Rotorcraft and Powered Lift Aircraft Forum, Bristol (Great Britain), September 1980,and Vertica, Vol. 5, 1981, pp. 35-63

13. Szechenyi E. , Tourjansky N. , "Stress Pattern Analysis Research at ONERA", AFARP 6 paper, RAE meeting , Farnborough (G.B.), March 1989

14. Paluch B., "Instumentation des maquettes de pales d'helicoptères en jauges de contrainte et capteurs de pression", I.M.F.L. Report N° 89/30, October 1989, 26 pages

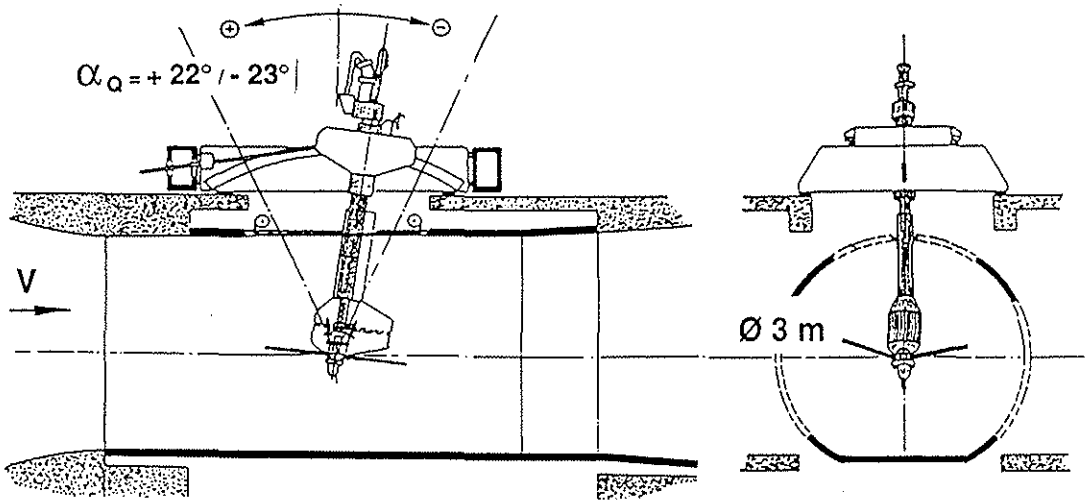

Fig. 1 : Rotor bench test in S2ch wind-tunnel.

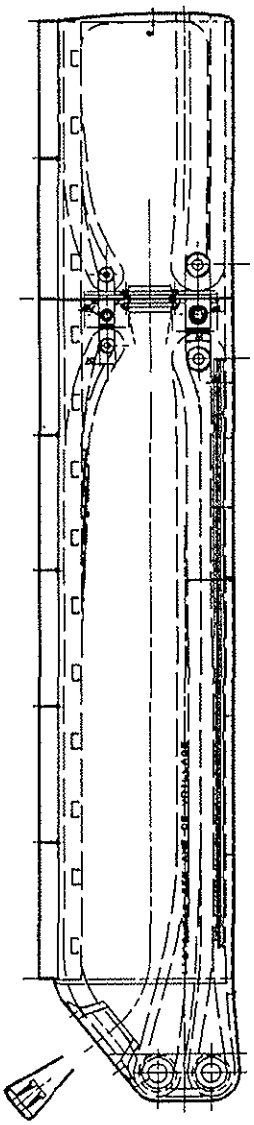

Fig. 2 :
Internal stucture of the blade.

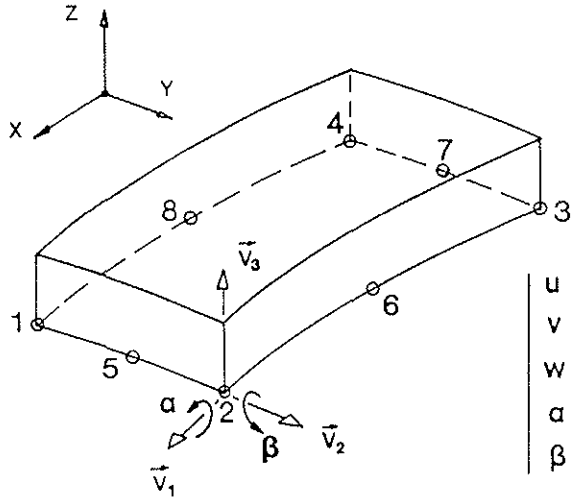

Fig. 3 : Thick composite shell element.

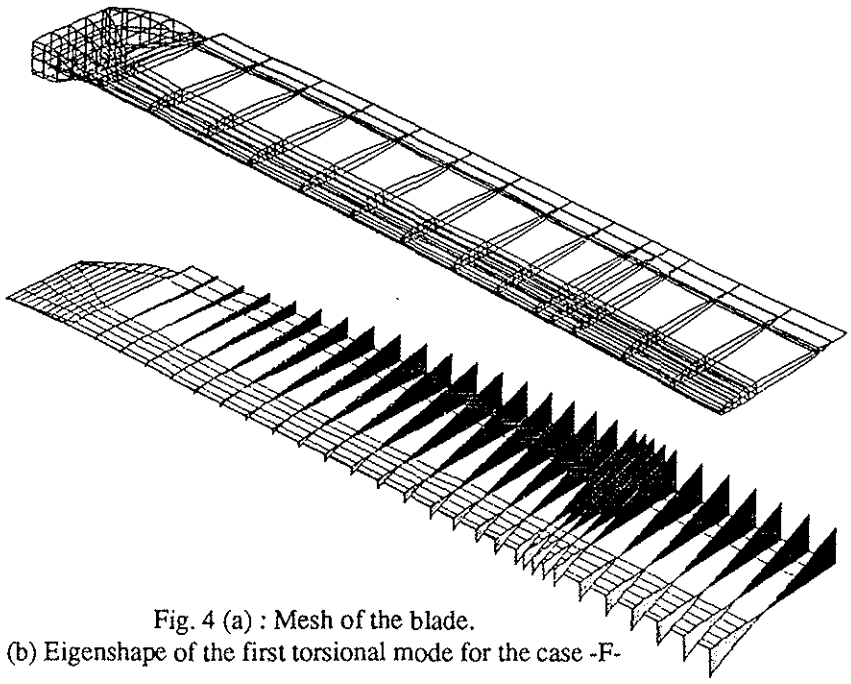

Fig. 4 (a) : Mesh of the blade.
(b) Eigenshape of the first torsional mode for the case -F-

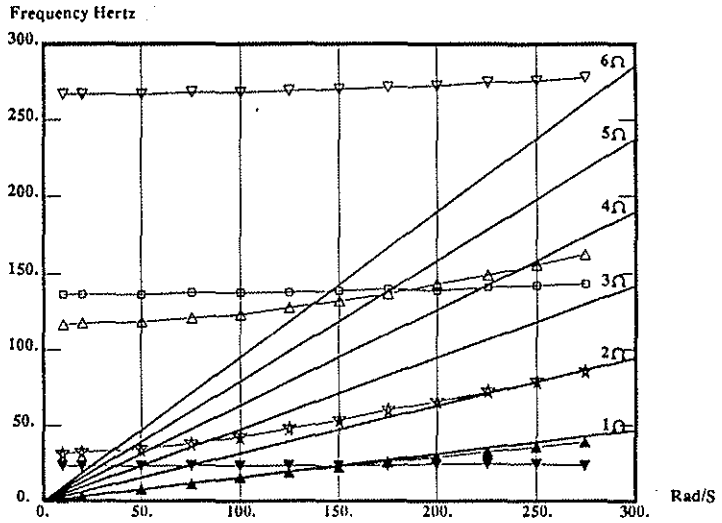

Fig. 5 : Variation of the first six natural computed frequencies of the flexible blade model with rotational speed -case B-

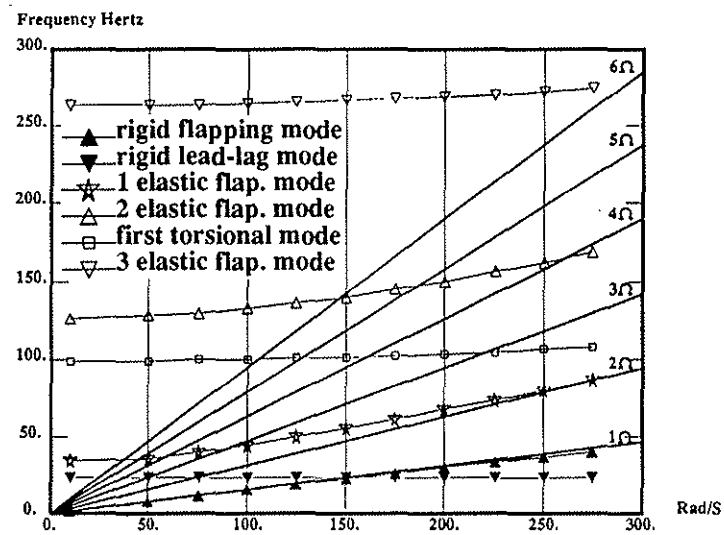

Fig. 6: Variation of the first six natural computed frequencies of the flexible blade model with rotational speed -case F-

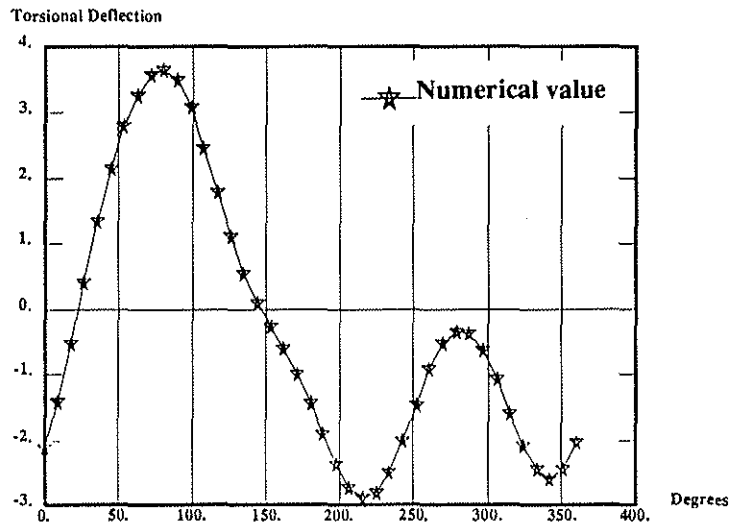

Fig. 7 : Evolution of the torsional deflection at the tip, for one complete cycle -case F-

Fig. 8 **LIFT COEFFICIENT CONTOURS**

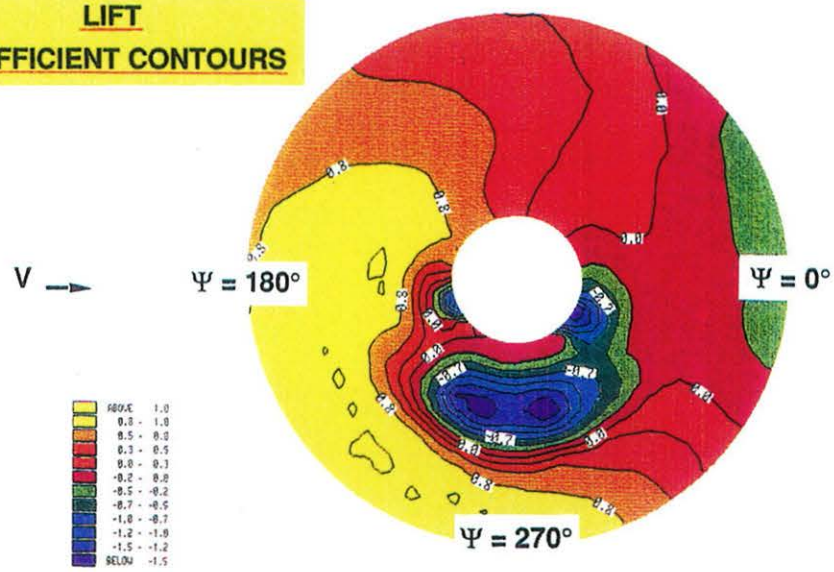

Fig. 9 **LOCAL INCIDENCE COEFFICIENT CONTOURS**

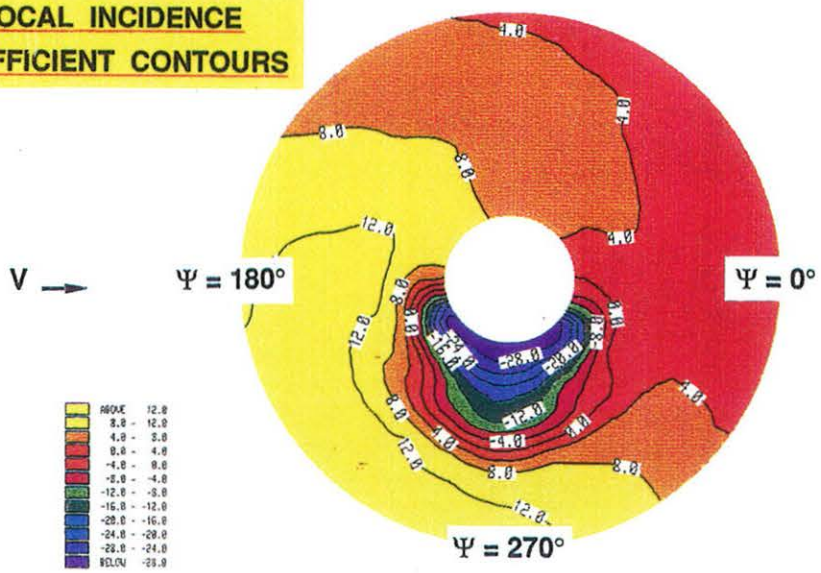

Fig. 10 **PITCHING MOMENT COEFFICIENT CONTOURS**

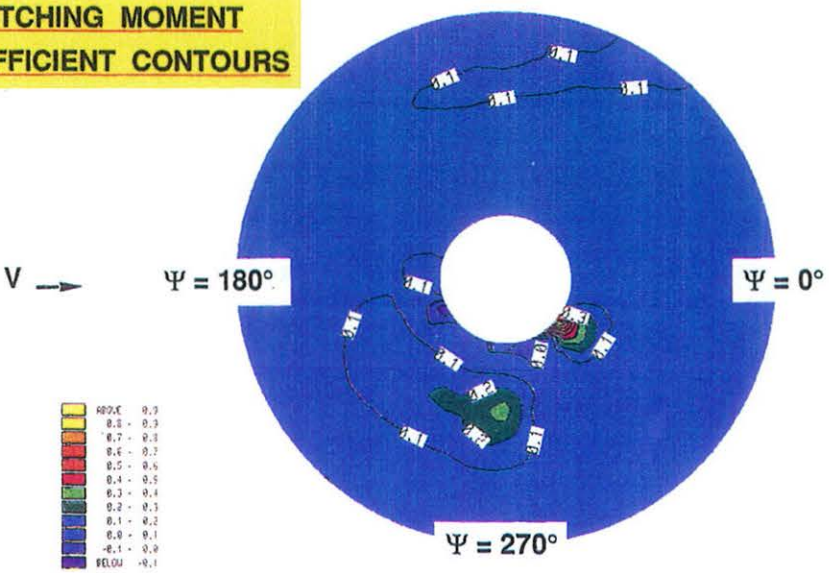

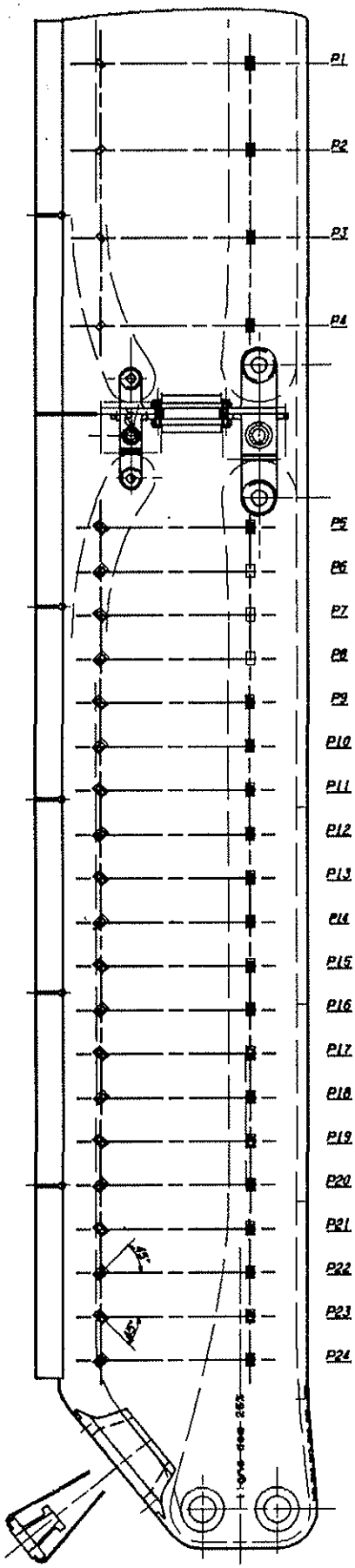

Fig. 11 : Strain gauge bridges distribution along the spanwise of the blade.

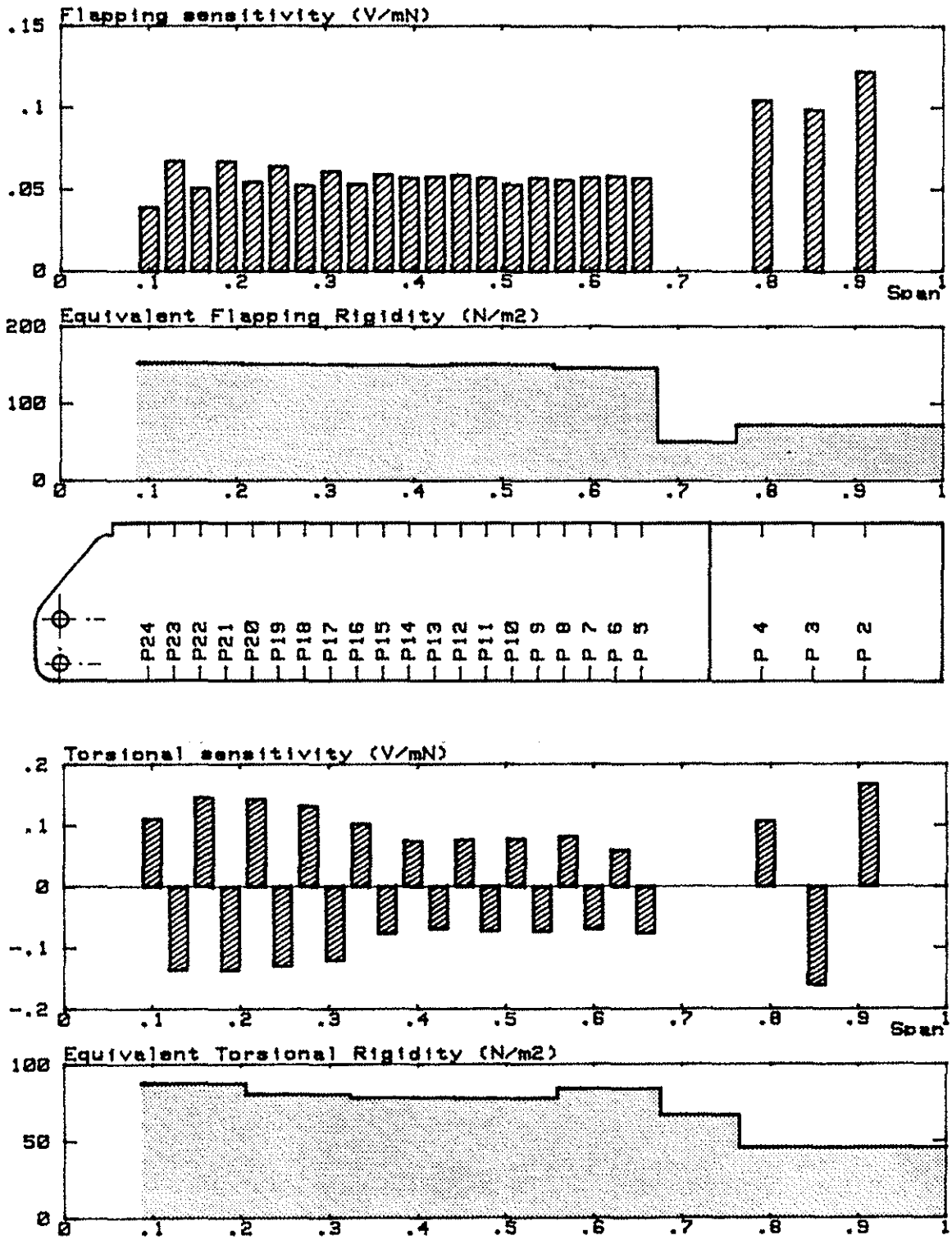

Fig. 12 : Flapping and torsional sensitivities of the strain gauge bridges.